# Joint-Denoise-and-Forward Protocol for Multi-Way Relay Networks

Ronald Y. Chang, Sian-Jheng Lin, and Wei-Ho Chung
Research Center for Information Technology Innovation, Academia Sinica, Taiwan
Email: {rchang, sjlin, whc}@citi.sinica.edu.tw

***Abstract*— This paper considers a multi-way relay network in which multiple users intend to achieve full information exchange with one another with the aid of a single relay. The denoise-and-forward (DNF) protocol with binary physical-layer network coding (PNC) is considered. A novel denoising scheme is proposed which does not require any modification on the communication mechanism of the original DNF protocol but only exploits the correlation among multiple received signals at the relay. The decision regions and denoise mapping for the proposed scheme and the original scheme are illustrated and compared for an exemplary three-way relay network. Simulation results verify the efficacy of the proposed scheme in achieving improved user decoding performance.**

***Index Terms*— Physical-layer network coding, denoise-and-forward, multi-way relay networks.**

## I. Introduction

In the classical two-way relay network, the denoise-and-forward (DNF) protocol adopting physical-layer network coding (PNC) [1]–[4] uses two phases to complete information exchange between two users through a single relay. Suppose that the two users' source bits are $S_1$ and $S_2$ which are modulated with binary phase shift keying (BPSK) as $X_1$ and $X_2$. In the first phase (the multiple access (MA) phase), user 1 transmits $X_1$ and user 2 transmits $X_2$ simultaneously to the relay. After receiving the noisy linear sum of $X_1 + X_2$, the relay performs *denoising* to estimate the XORed source bit $U = S_1 \oplus S_2$ and broadcasts it after modulation in the second phase (the broadcast (BC) phase). Essentially, the denoising performs a many-to-one mapping from the complex field operation in the wireless channel to the finite field operation for network coding [1]. Then, user 1 can decode user 2's information based on its own information $S_1$ and the XORed signal; same for user 2.

Due to its improved time efficiency (requires only two communication phases) and elegance, this idea has drawn significant attention since its inception. One generalization of the DNF protocol is applied to the multi-way relay network where multiple users intend to achieve full information exchange. A communication protocol for this scenario has been developed [5], [6], which adopts a pairwise user transmission scheme in the MA phase. The protocol involves several transmission time slots (as opposed to one for two-way relaying) in each phase, and traditionally the denoising is performed independently across different time slots. In this paper, we observe that there is a correlation among the transmitted signals in different time slots in the MA phase, which can be exploited by a joint denoising scheme to yield better denoising decisions. The proposed joint-DNF (JDNF) protocol retains the same time efficiency and signaling requirements of the DNF protocol, with improved user decoding performance as demonstrated numerically.

This paper is organized as follows. Sec. II presents the conventional DNF protocol. The proposed JDNF protocol is described in Sec. III. Performance results are presented in Sec. IV. Conclusion is given in Sec. V.

This work was supported in part by the National Science Council, Taiwan, under grant NSC 102-2218-E-001-001.

## II. The Conventional Denoise-and-Forward (DNF) Protocol

We consider a multi-way relay network with $K$ ($K \geq 2$) users where each user's message is intended for all other users and a full information exchange is desired. The DNF protocol consists of MA and BC phases, as described below. For simplicity, we assume unit channel gains for all links and perfect synchronization between signals simultaneously transmitted in the MA phase. BPSK signaling is considered for all transmissions. The users and the relay each have a single antenna.

*The MA phase:* The MA phase consists of $K-1$ time slots. In each time slot in the MA phase, a selected subset of $K$ users are scheduled to transmit concurrently to the relay. Let $g_{j,i} \in \{0,1\}$ indicate whether user $i$ transmits in the $j$th time slot. The received signal at the relay in the $j$th ($j = 1,\ldots,K-1$) time slot can therefore be represented as $Y_{R,j} = \sum_{i=1}^{K} g_{j,i}X_i + Z_{R,j}$, where $X_i$ is the BPSK signal that maps from user $i$'s source bit $S_i$ according to $X_i = 2S_i - 1$, and $Z_{R,j}$ is Gaussian noise with variance $\sigma^2$. The total received signals at the relay during the $K-1$ time slots can be represented in the form

$$\mathbf{Y}_R = \underbrace{\begin{bmatrix} g_{1,1} & g_{1,2} & \cdots & g_{1,K} \\ g_{2,1} & g_{2,2} & \cdots & g_{2,K} \\ \vdots & \vdots & \cdots & \vdots \\ g_{K-1,1} & g_{K-1,2} & \cdots & g_{K-1,K} \end{bmatrix}}_{\mathbf{G}:(K-1)\times K} \mathbf{X} + \mathbf{Z}_R \qquad (1)$$

where $\mathbf{Y}_R = [Y_{R,1}, Y_{R,2}, \ldots, Y_{R,K-1}]^T$, $\mathbf{X} = [X_1, X_2, \ldots, X_K]^T$, and $\mathbf{Z}_R = [Z_{R,1}, Z_{R,2}, \ldots, Z_{R,K-1}]^T$. The binary matrix $\mathbf{G}$ specifies the transmission scheduling for the protocol and its structure is made available to all users before communication.

After receiving the noisy combined signal, the relay makes the maximum *a posteriori* (MAP) estimate of $U_j = \bigoplus_{i=1}^{K} g_{j,i} S_i$, where $\bigoplus$ denotes the modulo-2 sum, from $Y_{R,j}$, i.e.,

$$\hat{U}_j = \underset{b=0,1}{\operatorname{argmax}}\ f_{Y_{R,j}}(y|U=b)P(U=b) \qquad (2)$$

where $f_{Y_{R,j}}(y|U=b)$ is the conditional probability distribution of the $j$th received signal at the relay given the $j$th modulo-2 sum. This method is referred to as *independent denoising* in this paper, as the denoised signal is determined independently across different transmission time slots.

*The BC phase:* The BC phase consists of $K-1$ time slots. In each time slot in the BC phase, the relay broadcasts the modulated denoised signal $X_{R,j} = 2\hat{U}_j - 1$ to all users. The received signal at user $i$ in the $j$th ($j = 1, \ldots, K-1$) time slot is given by $Y_{i,j} = X_{R,j} + Z_{i,j}$, where $Z_{i,j}$ is Gaussian noise with variance $\sigma^2$.

After the BC phase, each user $i$ decodes the information of all other users, i.e., $S_j, \forall j \neq i$, by using $Y_{i,1}, \ldots, Y_{i,K-1}$ and its own information $S_i$, with the knowledge of the logical form of $U_1, \ldots, U_{K-1}$. For successful decoding at each user side, $K-1$ linearly independent pieces of information about other users must be collected at the relay and further broadcasted. Since the $i$th column of $\mathbf{G}$ corresponds to the transmission of user $i$'s own information in the MA phase, $\mathbf{G}$ should have full rank after the $i$th column is removed, for $i = 1, \ldots, K$. This requires each row of $\mathbf{G}$ to contain at least two 1's. Since the number of 1's in $\mathbf{G}$ is proportional to the total number of transmissions, it is useful to consider each row of $\mathbf{G}$ containing exactly two 1's for energy conservation. For example, in a four-way relay network ($K = 4$), $\mathbf{G}$ may take various forms such as

$$\mathbf{G}_1 = \begin{bmatrix} 1 & 1 & 0 & 0 \\ 0 & 1 & 1 & 0 \\ 0 & 0 & 1 & 1 \end{bmatrix}, \quad \mathbf{G}_2 = \begin{bmatrix} 1 & 1 & 0 & 0 \\ 1 & 0 & 1 & 0 \\ 1 & 0 & 0 & 1 \end{bmatrix}. \qquad (3)$$

With this construction of $\mathbf{G}$, the independent denoising becomes a direct extension of the denoising in two-way relaying, where (2) reduces to [4]

$$\hat{U}_j = \begin{cases} 1, & |Y_{R,j}| \leq 1 + (\sigma^2 \ln 2)/2 \\ 0, & \text{otherwise} \end{cases}. \qquad (4)$$

The decision rule in (4) is depicted in Fig. 1.

## III. The Proposed Joint-Denoise-and-Forward (JDNF) Protocol

### A. A Motivating Example

It can be easily shown that, with the considered structure of $\mathbf{G}$, there is at least one column of $\mathbf{G}$ that contains more than one 1's, or equivalently, at least one user will transmit more than once in the MA phase. This creates correlation among the multiple received signals $Y_{R,1}, Y_{R,2}, \ldots, Y_{R,K-1}$ at the relay. Consider an example with $K = 3$ where the protocol adopts

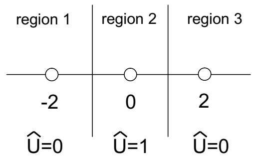


Fig. 1. Decision regions and denoise mapping in (4).

a user scheduling specified by

$$\mathbf{G} = \begin{bmatrix} 1 & 1 & 0 \\ 0 & 1 & 1 \end{bmatrix}. \qquad (5)$$

Thus, the relay receives $Y_{R,1} = X_1 + X_2 + Z_{R,1}$ and $Y_{R,2} = X_2 + X_3 + Z_{R,2}$ in the MA phase. Clearly, there is correlation between $Y_{R,1}$ and $Y_{R,2}$ and one signal gives some information about the other. To more explicitly motivate exploiting this correlation in the decision on $\hat{U}_j$, consider the case that the received signal $Y_{R,1}$ falls in region 1 and $Y_{R,2}$ falls in region 3 in Fig. 1. First, we observe that this is not possible in the absence of noise (as this would imply $X_1 = X_2 = -1$ and $X_2 = X_3 = 1$), but possible in the presence of noise. Second, the independent denoising in (4) will produce $\hat{U}_1 = \hat{U}_2 = 0$ in this case which correspond to the transmitted signals being either $X_1 = X_2 = X_3 = -1$ or $X_1 = X_2 = X_3 = 1$. However, the more likely transmitted signals are in fact either $X_1 = -1, X_2 = -1, X_3 = 1$ or $X_1 = -1, X_2 = 1, X_3 = 1$, with the corresponding denoised signals being $\hat{U}_1 = 0, \hat{U}_2 = 1$ or $\hat{U}_1 = 1, \hat{U}_2 = 0$. As can be seen, this is different from what the independent denoising would produce. This motivates a better denoising rule by leveraging the inter-dependence between different transmissions in the MA phase.

### B. The Optimal Denoising Strategy

The optimal denoising strategy is to collect all the received signals at the relay in the MA phase and make a joint decision accordingly. For a general network with $K$ users, this decision rule, referred to as *joint denoising* in this paper, is given by

$$\begin{aligned} &(\hat{U}_1, \hat{U}_2, \ldots, \hat{U}_{K-1}) \\ &= \underset{(b_1,\ldots,b_{K-1})\in\{0,1\}^{K-1}}{\operatorname{argmax}} f_{Y_{R,1},\ldots,Y_{R,K-1}}\Big(y_1, \ldots, y_{K-1} \,\Big|\, U_1 = b_1, \ldots, U_{K-1} = b_{K-1}\Big) \\ &\quad \times P\Big(U_1 = b_1, \ldots, U_{K-1} = b_{K-1}\Big). \end{aligned} \qquad (6)$$

For example, in our three-way relaying example with user scheduling specified by (5), the optimal decision rule becomes a task of comparing the four hypotheses in (7), shown at the top of the next page.

For the operation of joint denoising the relay will store all the received data in the MA phase ($Y_{R,j}$'s) in a queue of size proportional to $K-1$ before performing denoising and broadcasting the denoised signals. The computational complexity of joint denoising is proportional to the number of hypotheses, i.e., $2^{K-1}$.

### C. Decision Regions and Denoise Mapping

Fig. 2 and Fig. 3 compare the decision regions and denoise mapping for independent denoising and joint denoising in

$$
\begin{aligned}
f_{Y_{R,1},Y_{R,2}}\Big(y_1, y_2 \,\Big|\, U_1 = 0, U_2 = 0\Big) &= \frac{1}{2}\Bigg[\frac{1}{\sqrt{2\pi\sigma^2}}e^{-(y_1+2)^2/2\sigma^2} \times \frac{1}{\sqrt{2\pi\sigma^2}}e^{-(y_2+2)^2/2\sigma^2} \\
&\quad + \frac{1}{\sqrt{2\pi\sigma^2}}e^{-(y_1-2)^2/2\sigma^2} \times \frac{1}{\sqrt{2\pi\sigma^2}}e^{-(y_2-2)^2/2\sigma^2}\Bigg] \\
f_{Y_{R,1},Y_{R,2}}\Big(y_1, y_2 \,\Big|\, U_1 = 0, U_2 = 1\Big) &= \frac{1}{2}\Bigg[\frac{1}{\sqrt{2\pi\sigma^2}}e^{-(y_1+2)^2/2\sigma^2} \times \frac{1}{\sqrt{2\pi\sigma^2}}e^{-y_2^2/2\sigma^2} \\
&\quad + \frac{1}{\sqrt{2\pi\sigma^2}}e^{-(y_1-2)^2/2\sigma^2} \times \frac{1}{\sqrt{2\pi\sigma^2}}e^{-y_2^2/2\sigma^2}\Bigg] \\
f_{Y_{R,1},Y_{R,2}}\Big(y_1, y_2 \,\Big|\, U_1 = 1, U_2 = 0\Big) &= \frac{1}{2}\Bigg[\frac{1}{\sqrt{2\pi\sigma^2}}e^{-y_1^2/2\sigma^2} \times \frac{1}{\sqrt{2\pi\sigma^2}}e^{-(y_2-2)^2/2\sigma^2} \\
&\quad + \frac{1}{\sqrt{2\pi\sigma^2}}e^{-y_1^2/2\sigma^2} \times \frac{1}{\sqrt{2\pi\sigma^2}}e^{-(y_2+2)^2/2\sigma^2}\Bigg] \\
f_{Y_{R,1},Y_{R,2}}\Big(y_1, y_2 \,\Big|\, U_1 = 1, U_2 = 1\Big) &= \frac{1}{2}\Bigg[\frac{1}{\sqrt{2\pi\sigma^2}}e^{-y_1^2/2\sigma^2} \times \frac{1}{\sqrt{2\pi\sigma^2}}e^{-y_2^2/2\sigma^2} \\
&\quad + \frac{1}{\sqrt{2\pi\sigma^2}}e^{-y_1^2/2\sigma^2} \times \frac{1}{\sqrt{2\pi\sigma^2}}e^{-y_2^2/2\sigma^2}\Bigg] \qquad (7)
\end{aligned}
$$

our three-way relaying example when the signal-to-noise ratio (SNR) is set to 0 dB and $-8$ dB, respectively. The SNR for all transmissions is defined as $1/\sigma^2$. As can be seen in Fig. 2(a) and Fig. 3(a), the decision regions for independent denoising are simply two orthogonal decision regions depicted in Fig. 1. When the SNR value decreases (or the noise variance increases), the decision boundaries shift away from $\pm 1$ according to (4), making the center white area larger. Note that Fig. 2(a) and Fig. 3(a) are analogous to the decision regions and denoise mapping for two-way relaying with quadrature phase shift keying (QPSK) signaling [2, Fig. 4], even though in our three-way relaying with BPSK there are only 3 bits of information exchanged in the network as opposed to 4 bits in two-way relaying with QPSK.

The interesting case is the joint denoising which shows different decision regions. As we discussed, the upper-left and lower-right regions are two impossible regions in the absence of noise. It turns out that the joint denoising scheme will merge these two regions into neighbor regions as shown in Fig. 2(b) and Fig. 3(b). Effectively, the joint denoising makes a better decision when $(Y_{R,1}, Y_{R,2})$ falls in these regions, leading to better average decoding performance at the user side (see Sec. IV). The joint denoising also exhibits more complex shapes of regions. If there were no correlation between different transmissions in the MA phase, the joint denoising becomes equivalent to the independent denoising, and the decision regions for both schemes are given by the plots for independent denoising. However, in the considered DNF protocol with minimum required communication time slots ($K-1$ for MA and $K-1$ for BC), there is always a correlation among different transmissions, as discussed previously. Note that these plots only show the decision regions but give no information on the probability of $(Y_{R,1}, Y_{R,2})$ falling in each region, which is however accounted for in calculating the average error performance for each scheme (Sec. IV).

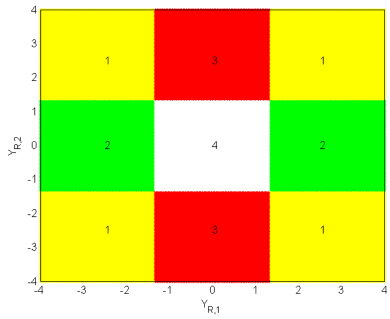


(a)

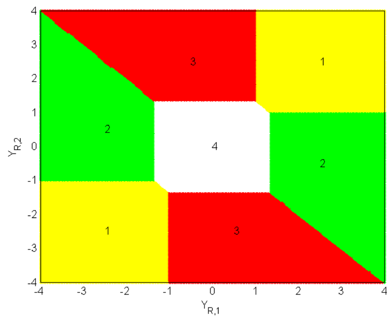


(b)

Fig. 2. Decision regions and denoise mapping for (a) independent denoising and (b) joint denoising for a three-way relay network with SNR = 0 dB, where the colors/numbers represent the denoise mappings as follows: yellow ("1"), $(\hat{U}_1, \hat{U}_2) = (0, 0)$; green ("2"), $(\hat{U}_1, \hat{U}_2) = (0, 1)$; red ("3"), $(\hat{U}_1, \hat{U}_2) = (1, 0)$; white ("4"), $(\hat{U}_1, \hat{U}_2) = (1, 1)$.

## IV. Performance Results and Discussions

In this section, we compare the user decoding performance when employing the conventional DNF protocol (with independent denoising) and the proposed JDNF protocol (with joint denoising) in the multi-way relay network. The simula-

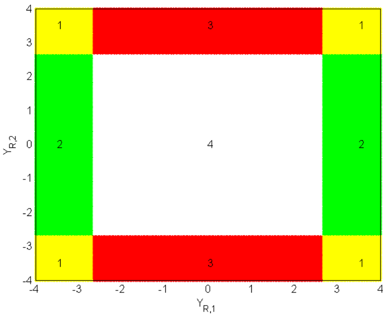

(a)

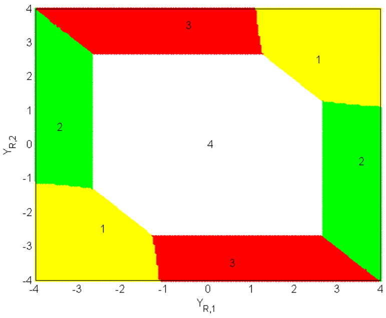

(b)

Fig. 3. Decision regions and denoise mapping for (a) independent denoising and (b) joint denoising for a three-way relay network with SNR $= -8$ dB, where the notations follow those in Fig. 2.

tion follows the system setting described in Sec. II. Fig. 4(a) compares the bit-error-rate (BER) performance in a three-way relay network. In this scenario, the scheduling matrix $\mathbf{G}$ can take only one form in the sense that one user will transmit twice and two users will transmit once (e.g., (5)). The JDNF protocol shows slight improvements over the DNF protocol. The improvement is a result of a better denoising decision made by JDNF when $(Y_{R,1}, Y_{R,2})$ falls in regions of different colors (e.g., the upper-left and lower-right regions in Figs. 2–3). When $(Y_{R,1}, Y_{R,2})$ falls in regions of identical colors, the same denoise signals will be broadcasted with both JDNF and DNF and therefore the same decoding performance will be yielded. Fig. 4(a) shows an average over different values of $(Y_{R,1}, Y_{R,2})$.

Fig. 4(b) compares the BER performance in a ten-way relay network. In this scenario, the scheduling matrix $\mathbf{G}$ can assume various forms. We consider two "extreme" schemes. In the first scheme (user scheduling 1), the transmission load is roughly evenly distributed among all users, with $\mathbf{G}$ having the "cascade" structure as in $\mathbf{G}_1$ in (3). In the second scheme (user scheduling 2), the transmission load is centered on one particular user, with $\mathbf{G}$ in the form of $\mathbf{G}_2$ in (3). First, we observe that user scheduling 2 yields a lower BER than user scheduling 1 in combination with DNF or JDNF. This is because user scheduling 1 suffers from a heightened error propagation effect in the sequential decoding of the other users. Second, we observe that the performance gain yielded

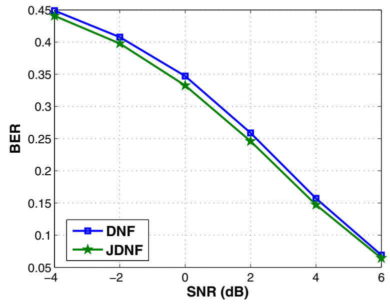


(a)

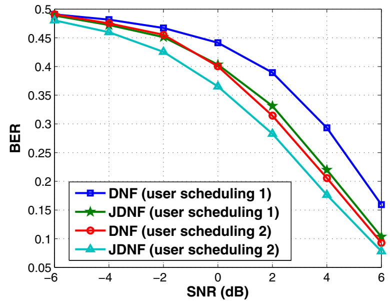


(b)

Fig. 4. BER performance for DNF and JDNF protocols. (a) 3-way relaying. (b) 10-way relaying.

by joint denoising increases with the number of users in the network. In addition, JDNF beats DNF by a greater margin if the original DNF protocol has poorer performance (with user scheduling 1).

## V. Conclusion

A new DNF-type protocol has been proposed for multi-way relay networks with the objective of facilitating full information exchange in the network. The proposed scheme retains the information exchange mechanism of the original DNF protocol but exploits the correlation among multiple received signals at the relay in making improved denoise decision at the relay. The decision regions and denoise mapping for the proposed scheme and the original scheme are compared for a three-way relay network. Under the setting of moderate-sized and larger-sized networks, the proposed protocol demonstrated various degrees of improved decoding performance through simulation results.

## References


[1] S. Zhang, S. C. Liew, and P. P. Lam, "Hot topic: Physical-layer network coding," in *Proc. ACM MobiCom*, Los Angeles, CA, Sept. 2006, pp. 358–365.

[2] P. Popovski and H. Yomo, "The anti-packets can increase the achievable throughput of a wireless multi-hop network," in *Proc. IEEE ICC*, Istanbul, Turkey, June 2006, pp. 3885–3890.

[3] ——, "Wireless network coding by amplify-and-forward for bi-directional traffic flows," *IEEE Commun. Lett.*, vol. 11, no. 1, pp. 16–18, Jan. 2007.

[4] B. Nazer and M. Gastpar, "Reliable physical layer network coding," *Proc. IEEE*, vol. 99, no. 3, pp. 438–460, Mar. 2011.

[5] L. Ong, C. M. Kellett, and S. J. Johnson, "Capacity theorems for the AWGN multi-way relay channel," in *Proc. IEEE ISIT*, Austin, TX, June 2010, pp. 664–668.

[6] L. Ong, S. J. Johnson, and C. M. Kellett, "The capacity region of multiway relay channels over finite fields with full data exchange," *IEEE Trans. Inform. Theory*, vol. 57, no. 5, pp. 3016–3031, May 2011.